

Study on a Novel Methodology for Developing the Skeletal Mechanism of RP-3 Aviation Kerosene

Ping Liu, Xiangkui Gong, Tao Deng, and Jin Yu*

Cite This: *ACS Omega* 2023, 8, 37282–37292

Read Online

ACCESS |



Metrics & More

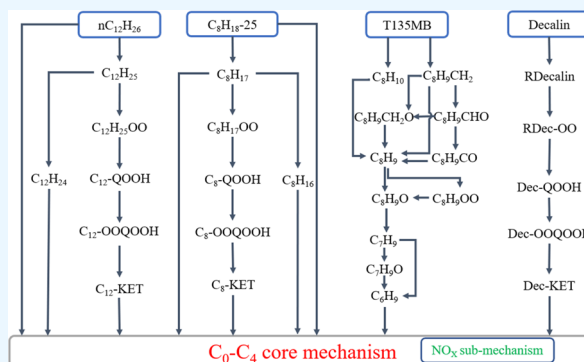


Article Recommendations



Supporting Information

ABSTRACT: An urgent requirement for high-precision numerical simulation of modern aero-engines is the development of a highly simplified and accurate reaction mechanism for aviation kerosene. However, there is still lack of a reduced mechanism that can effectively capture the low- and high-temperature characteristics of RP-3 aviation kerosene. In light of this, in this study, a novel methodology for developing skeletal mechanism by combining the detailed C_0 – C_4 mechanism and C_5 – C_n high-carbon molecular skeletal mechanism was proposed and applied. To construct the RP-3 skeletal mechanism, a surrogate fuel consisting of 54% *n*-dodecane, 22% 2,5-dimethylhexane, 14% 1,3,5-trimethylbenzene, and 10% decalin was utilized. Based on the proposed methodology, a skeletal mechanism comprising 153 species and 858 reactions has been developed. Various combustion characteristics of each surrogate component and the RP-3 aviation kerosene, such as the ignition delay, concentration of material components, laminar flame, and NO emission, were examined to validate the developed mechanism. The proposed methodology in this study offers a novel approach to develop mechanisms for high-carbon fuels. Additionally, the developed skeletal mechanism serves as a foundation for the design and optimization of aero-engines.



1. INTRODUCTION

The worldwide energy and environmental crises are of utmost concern, and as a result, safety, high efficiency, and low-carbon environmental protection have become the primary focus of aero-engine design optimization. Improving the combustion efficiency of aero-engine combustors and reducing pollutant emissions have become urgent issues for the development of new-generation aero-engines. Therefore, it is imperative to conduct fluid dynamics calculations (CFD) that couple reaction dynamics mechanisms to the combustion process of aviation fuel in aero-engines in order to provide strong support for aero-engine design and optimization. However, the composition of aviation fuel is exceedingly complex, and constructing the chemical reaction mechanism of all components for numerical simulation research is nearly impossible under the current conditions. As a solution, the surrogate fuel, which selects a few typical representative components to simulate the physical and chemical properties of real fuels, has become an effective approach.

As the most widely used aviation fuel in China, RP-3 aviation kerosene has garnered increasing attention from researchers. Various studies have been conducted to construct the reaction mechanism of the RP-3 surrogate fuel. Zhang et al.,¹ Mao et al.,² and Zheng et al.³ have, respectively, developed detailed chemical reaction mechanisms for RP-3 aviation kerosene's two-component, three-component, and four-com-

ponent surrogate fuels. These surrogate fuel models can better simulate the ignition characteristics of RP-3 aviation kerosene.

Although the above-mentioned detailed reaction mechanisms for RP-3 aviation kerosene provide accurate fuel oxidation combustion details, the multidimensional combustion simulation using this mechanism requires a considerable amount of computational resources and time. This makes it challenging to accept and use with current computing resources. Therefore, developing reduced or skeletal mechanisms with a compact structure and reliable performance is crucial to realizing an efficient combustion simulation. Several researchers have attempted to obtain reduced mechanisms for RP-3 at high-temperature combustion condition. For instance, Zeng et al.⁴ developed a reduced mechanism that includes 150 species and 590 reactions. Liu et al.⁵ obtained an RP-3 surrogate mechanism with 59 species and 158 reactions by using various mechanism reduction schemes.

Although the reduced mechanism described above has greatly facilitated numerical simulation research of aviation

Received: July 15, 2023

Accepted: September 19, 2023

Published: September 29, 2023



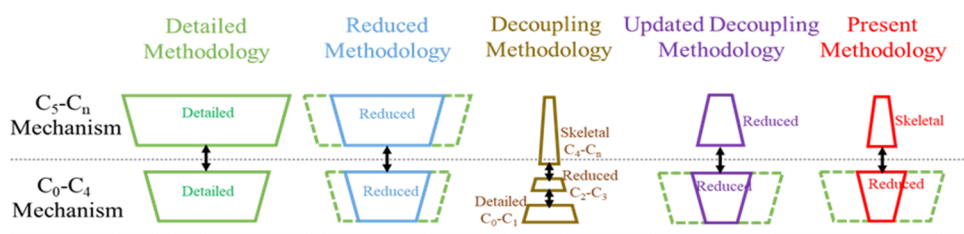


Figure 1. Different methods for contrast diagram.

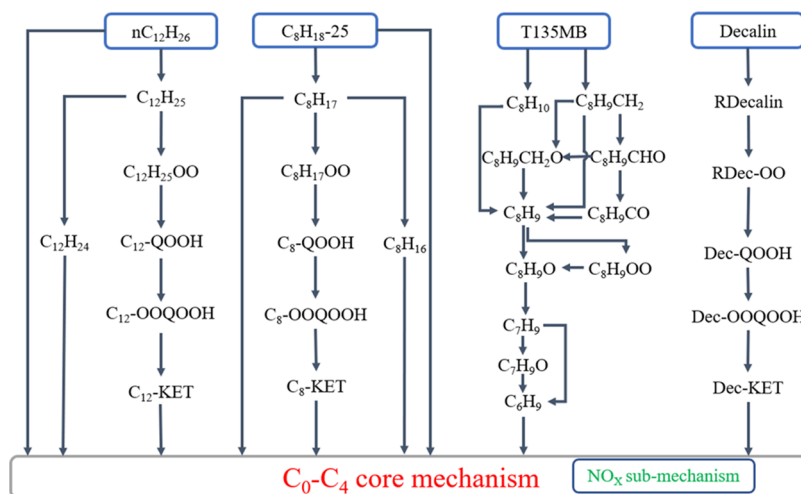


Figure 2. Main reaction path model of the fuel.

kerosene combustion, it is primarily aimed at high-temperature reaction conditions of flame propagation, with few reports on the reduced mechanism that reflects low-temperature ignition characteristics. Ranzi et al.⁶ proposed the utilization of lumping procedures and reduction methods to derive the skeletal mechanism for 231 species of aviation kerosene. This approach significantly decreases the size of the mechanism in comparison to the detailed one. Nevertheless, the resulting species mechanism remains too extensive for practical applications in CFD simulations. Currently, Liu et al.⁷ and Liu et al.⁸ have, respectively, developed the three-component and four-component surrogate fuel skeletal mechanisms of RP-3 aviation kerosene based on the decoupling methodology.⁹ However, the product distribution of combustion intermediate species is the most significant influencing factor affecting the combustion radical pool, which, in turn, affects the phenomenological behavior of combustion kinetics of fuels.¹⁰ Zhang and Sarathy¹¹ indicated that the C_2 – C_3 reduction mechanism and the C_4 – C_n skeletal mechanism in the decoupling method cannot accurately describe the reactions of various key intermediate species. Therefore, although the construction of the skeletal mechanism using the decoupling method is simplified, its accuracy still needs improvement. Additionally, the currently developed reaction mechanism of RP-3 aviation kerosene lacks the construction of the formation mechanism of nitrogen oxides, which limits research on its pollutant emissions.

In order to address the issue of the accuracy of the decoupling methodology, this study presents a novel approach for constructing skeletal mechanisms. By utilizing this new method, a skeletal reaction mechanism for RP-3 aviation kerosene, which is suitable for both high- and low-temperature conditions, was developed and the NO_x generation mechanism

was integrated. The validity of the mechanism was subsequently confirmed through extensive experimental data.

2. METHODOLOGY OF CONSTRUCTING SKELETAL MECHANISM

2.1. Theory for Methodology. Currently, there are various approaches available for the development of compact reaction mechanisms that are suitable for CFD simulations, as depicted in Figure 1. The most commonly used approach is the mechanism reduction method, which involves the elimination of unnecessary components and reactions from the detailed mechanism under specific conditions. However, for high-molecular-weight fuels, the size of the resulting reduced mechanism is still too large to be applied to CFD simulations. Another approach is the decoupling methodology, where the mechanism is primarily composed of three parts: the C_0 – C_3 core mechanism, consisting of the detailed C_0 – C_1 mechanism, and the reduced C_2 – C_3 mechanism, and the C_4 – C_n submechanism. This methodology can lead to the development of a reaction mechanism with an extremely compact size, but its accuracy still needs to be improved. To address this issue, Zhang and Sarathy et al.¹¹ adopted an upgraded decoupling methodology, which involves integrating the detailed C_0 – C_4 core mechanism and the reduced C_5 – C_n mechanism to develop a small-scale high-temperature chemical reaction mechanism. However, this method still faces challenges in developing a compact, low-temperature reaction mechanism.

Therefore, this paper proposes a novel methodology that combines the compactness of the decoupling methodology and the high precision of the upgraded decoupling methodology to develop a skeletal reaction mechanism for the RP-3 surrogate fuel. The primary strategy of this methodology is as follows:

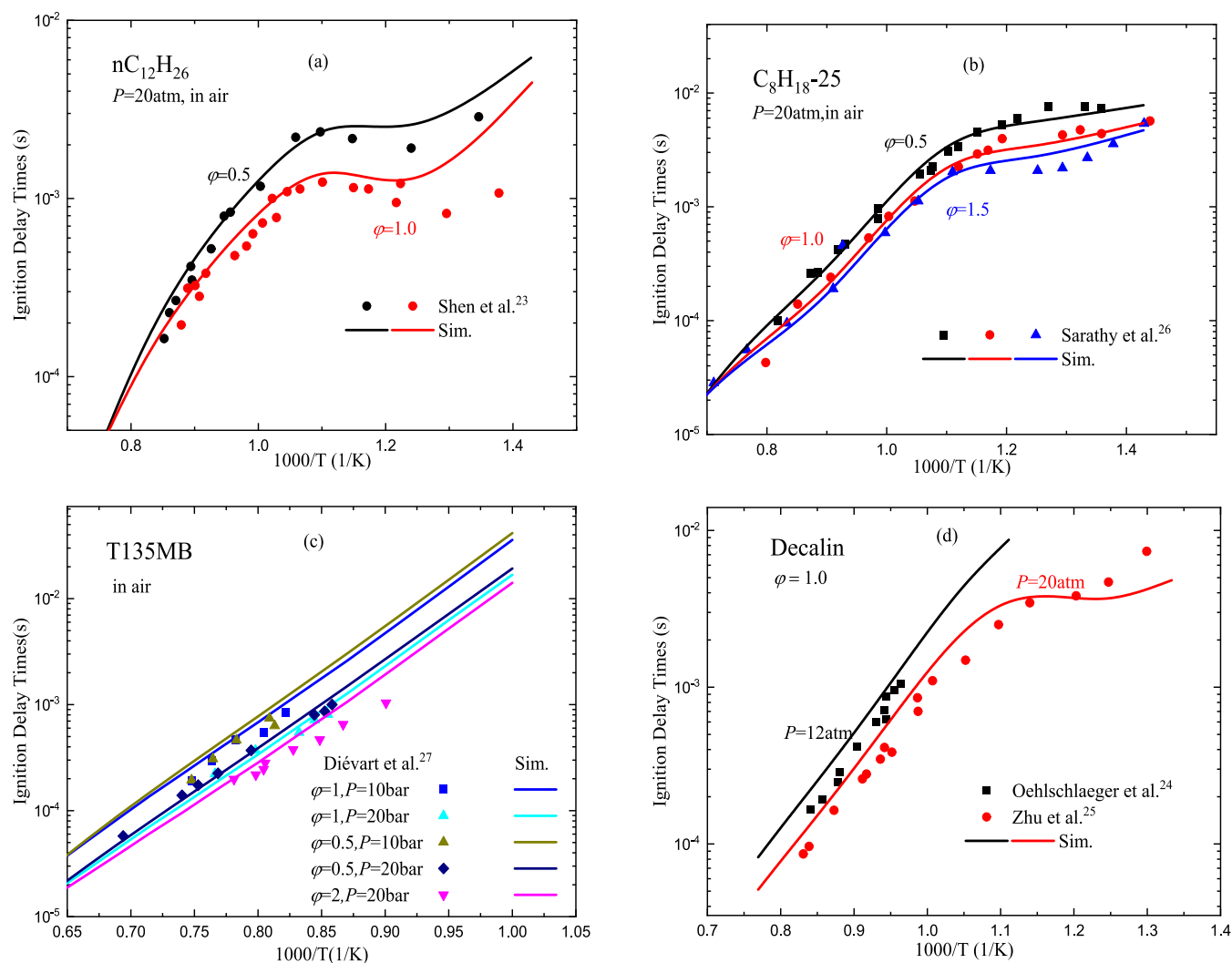


Figure 3. Comparison between surrogate mechanism predicted values and experimental data of ignition delay time for (a) *n*-dodecane, (b) 2,5-dimethylhexane, (c) 1,3,5-trimethylbenzene, and (d) decalin. Symbols represent the experimental values.^{23–27} Solid lines represent the computational values of surrogate mechanism.

(1) construct the C_5 – C_n high-carbon molecular skeletal mechanism of the fuel based on the detailed C_0 – C_4 mechanism; (2) optimize the reaction coefficient of the C_5 – C_n skeletal mechanism using experimental data; (3) eliminate redundant species and reactions in the detailed mechanism of C_0 – C_4 through mechanism simplification. In this new methodology, the C_5 – C_n skeletal submechanism reduces the overall size of the reaction mechanism, while the detailed C_0 – C_4 core mechanism contains abundant key species and reactions that can improve the prediction accuracy.

2.2. Developing of Reaction Mechanism. Based on the idea of directly matching the molecular structure and functional groups,^{12–14} *n*-dodecane ($nC_{12}H_{26}$), 2,5-dimethylhexane (C_8H_{18-25}), 1,3,5-trimethylbenzene (T135MB), and decalin were selected as the surrogate components. The formulation of surrogate fuel was determined by matching four functional groups: CH_3 , CH_2 , CH , and phenyl. The mole fractions used were 54% $nC_{12}H_{26}$, 22% C_8H_{18-25} , 14% T135MB, and 10% decalin. For a detailed explanation of the surrogate fuel selection and proportion determination, refer to ref 15.

Using the new methodology, the skeletal mechanism of the RP-3 surrogate fuel was constructed. The main reaction path of the mechanism is shown in Figure 2. The AramcoMech 3.0 mechanism¹⁶ was selected as the core mechanism for C_0 – C_4 . The high-temperature direct cracking pathway of paraffins was added based on the reaction pathways of *n*-dodecane and iso-octane by Fang et al.¹⁷ and Chang et al.,⁹ and the intermediate species of high-temperature cracking were optimized to obtain the skeletal mechanism of $nC_{12}H_{26}$ and C_8H_{18-25} . The C_4 – C_n skeletal mechanism of T135MB mainly refers to the reaction pathway constructed by Liu et al.,⁷ while the C_5 – C_n skeletal mechanism of decalin mainly refers to the reaction pathway constructed by Fang et al.¹⁷ Additionally, C_6H_6 , an important substance for pyrolysis, was added to the C_5 – C_n skeletal mechanism of decalin. The C_4 species and related reactions were added to the mechanism of the four components to improve the prediction accuracy of the mechanism. Finally, the NO_x generation mechanism in GRI 3.0¹⁸ was coupled to the skeletal mechanism to obtain the final coupled skeletal mechanism of RP-3 surrogate fuel.

The directed relation graph with error propagation (DRGEP)¹⁹ method was utilized to reduce the C_0 – C_4

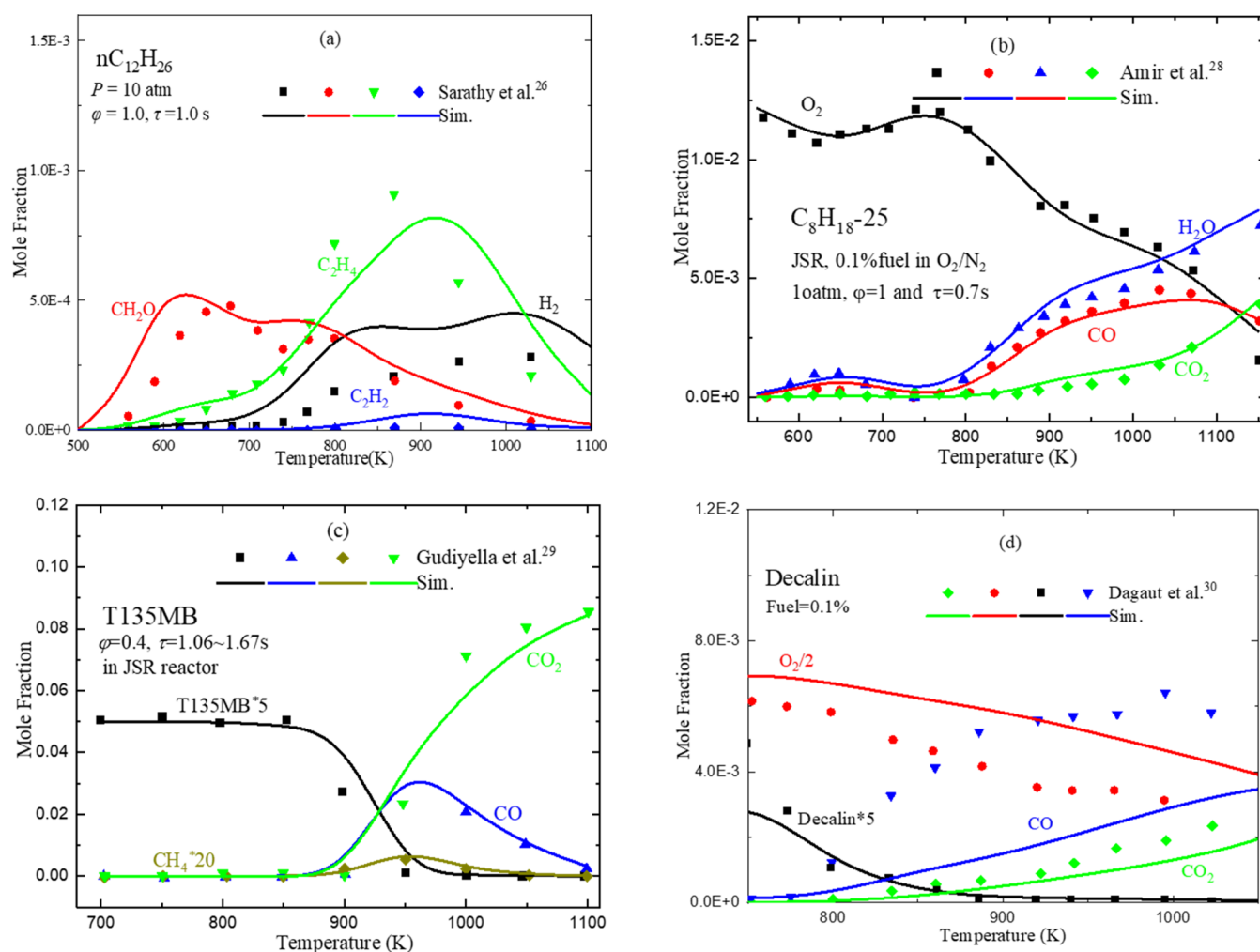


Figure 4. Comparison between surrogate mechanism predicted values and experimental data of species molar fraction distribution for (a) *n*-dodecane, (b) 2,5-dimethylhexane, (c) 1,3,5-trimethylbenzene, and (d) decalin. Symbols represent the experimental values.^{24,28–30} Solid lines represent the computational values of the surrogate mechanism.

mechanism, followed by the full species sensitivity analysis (FSSA)²⁰ for further reduction. Both methods utilize the ignition delay time as a target parameter, with reaction conditions set at equivalence ratio $\phi = 0.5–2$, pressure $P = 1–50$ atm, and temperature $T = 700–1800$ K. The selection of initial retained species has a significant impact on the final reduction effect. In this study, OH, HO₂, CO, and CH₂O were selected as retained species, in addition to the initial fuel, oxygen, and final products, to better preserve the low-temperature reaction mechanism.²¹ H radicals and other high flame speed-sensitive substances such as CH₄ of T135MB and C₂H₂ of decalin were also used as retained species to improve the prediction accuracy for high-temperature flames. Similar to the reduction strategy of the C₀–C₄ mechanism, the detailed NO_x reaction chemistry has been reduced by DRGEP and FSSA. NO and NO₂ were selected as retained species. The reduction process prioritized maintaining high accuracy for each mechanism of component, followed by coupling the mechanisms of component to obtain the RP-3 skeletal mechanism consisting of 153 species and 858 reactions. This surrogate skeletal mechanism is provided in the [Supporting Information](#).

3. CANDIDATE COMPONENT MECHANISM VALIDATION

The multicomponent surrogate mechanism should accurately describe the combustion characteristics of each component before the validation of describing the surrogate mixture combustion process. Therefore, this section focuses on verifying the mechanism of each surrogate component in fundamental combustion experiments. The combustion process with surrogate fuel was simulated using the CHEMKIN software.²² The validation process includes assessing the ignition delay time, jet stirred reactor (JSR) component concentrations, and laminar flame speed to ensure comprehensive results.

3.1. Ignition Delay Time Validation. The ignition delay time simulation data for *n*C₁₂H₂₆, C₈H₁₈-25, T135MB, and decalin were compared with experimental data.^{23–27} The comparison between the simulated and experimental values is shown in [Figure 3](#). [Figure 3\(a\)](#) displays the comparison of the ignition delay time of *n*C₁₂H₂₆ with the experimental value for $\phi = 0.5$ and 1.0, respectively. It is evident that the skeletal mechanism of *n*C₁₂H₂₆ can accurately reflect the high- to low-temperature ignition characteristics. Due to the simplification of the skeletal mechanism, the accuracy of predictions in the low-temperature range (below 750 K) is compromised when ϕ

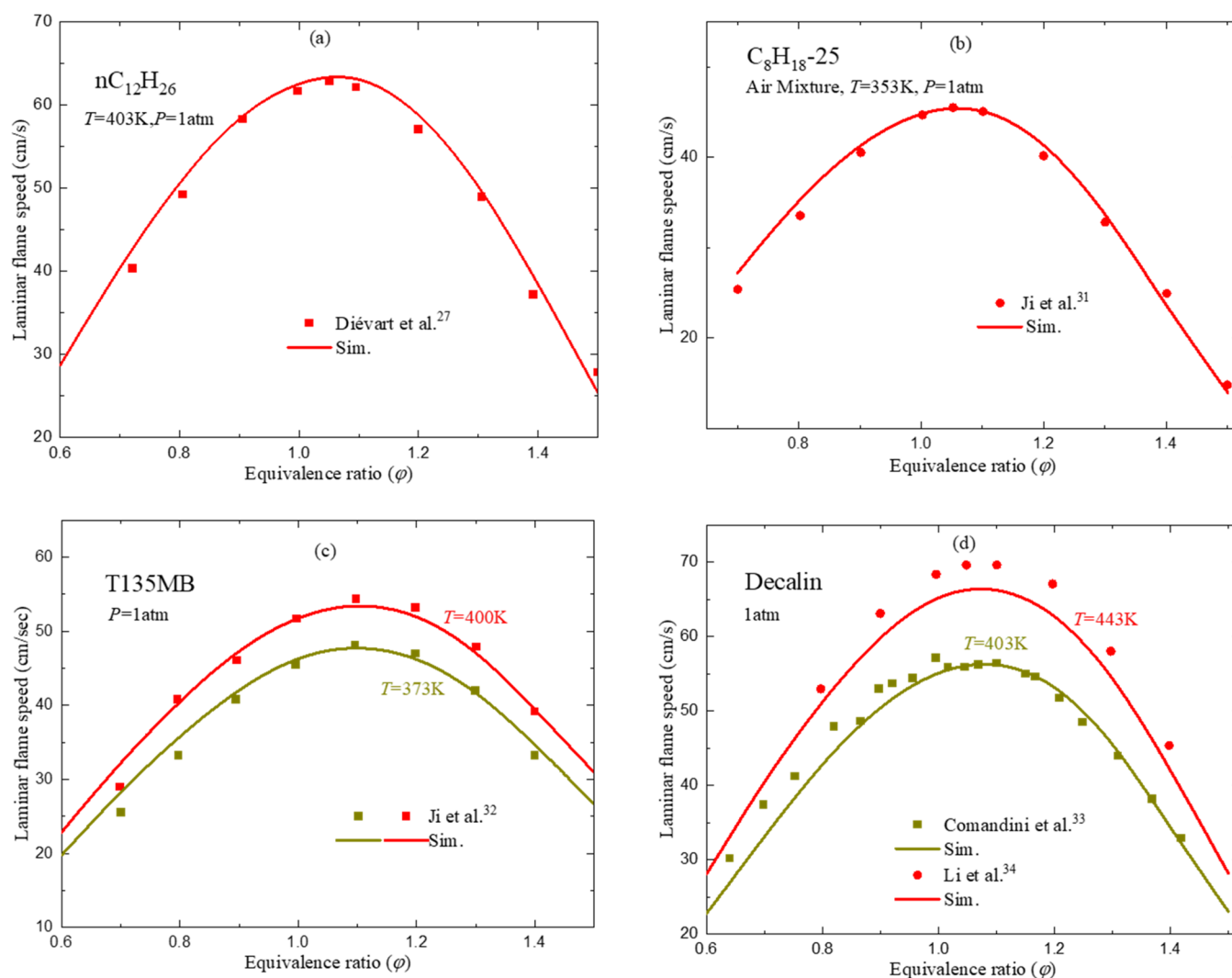


Figure 5. Comparison between surrogate mechanism predicted values and experimental data of laminar flame speed for (a) *n*-dodecane, (b) 2,5-dimethylhexane, (c) 1,3,5-trimethylbenzene, and (d) decalin. Symbols represent the experimental values.^{25,31–34} Solid lines represent the computational values of surrogate mechanism.

= 1.0. Figure 3(b) shows the variation in the ignition delay time of C_8H_{18-25} under equivalence ratios of 0.5, 1.0, and 1.5. The mechanism can predict the high- and low-temperature ignition delay times of C_8H_{18-25} with high precision, particularly for the NTC (negative temperature coefficient) phenomenon in the low-temperature region. Figure 3(c) demonstrates that under different pressures and equivalence ratios, the predicted ignition delay time of the T135MB mechanism in the high-temperature region agrees well with the experimental data. Figure 3(d) depicts that when the equivalence ratio is $\phi = 1.0$, and $P = 12$ and 20 atm, the predicted values of decalin in both high- and low-temperature regions are in good agreement with the experimental data.

3.2. Species Concentration Validation. The oxidation data of $nC_{12}H_{26}$, C_8H_{18-25} , T135MB, and decalin at various temperature ranges were used to verify the skeletal mechanism in a JSR. The intermediate species profiles of the four surrogate components were sufficiently validated. The JSR simulation data for these components were then compared with experimental data,^{24,28–30} and the results are presented in Figure 4(a–d). The analysis revealed that the $nC_{12}H_{26}$ mechanism in the surrogate mechanism accurately reflects

the concentration trend of H_2 , CH_2O , C_2H_4 , and C_2H_2 , and the predicted values are in good agreement with the experimental values. Similarly, the mechanism of C_8H_{18-25} accurately reflects the changing trends of the O_2 , H_2O , CO , and CO_2 , and it is in good agreement with the experimental values. The comparison between predictions and experimental data for T135MB is shown in Figure 4(c), and there is satisfactory agreement between predictions and experimental data on the concentrations of T135MB, CO , CO_2 , and CH_4 . Additionally, Figure 4(d) shows that the decalin mechanism correctly reflects the change trend of CO_2 and O_2 , but the error in the CO prediction is relatively large. Hence, there is potential for further enhancing the decalin mechanism to improve CO prediction. Overall, the results suggest that the skeletal mechanism of the four components has high accuracy in predicting JSR species concentrations.

3.3. Laminar Flame Speed Validation. Laminar flame speed is a critical parameter that provides valuable insights into fuel diffusivity, reactivity, and heat release. Hence, the laminar flame speeds of the four surrogate components were sufficiently validated. The comparison between the simulated and experimental values^{25,31–34} is presented in Figure 5. Figure

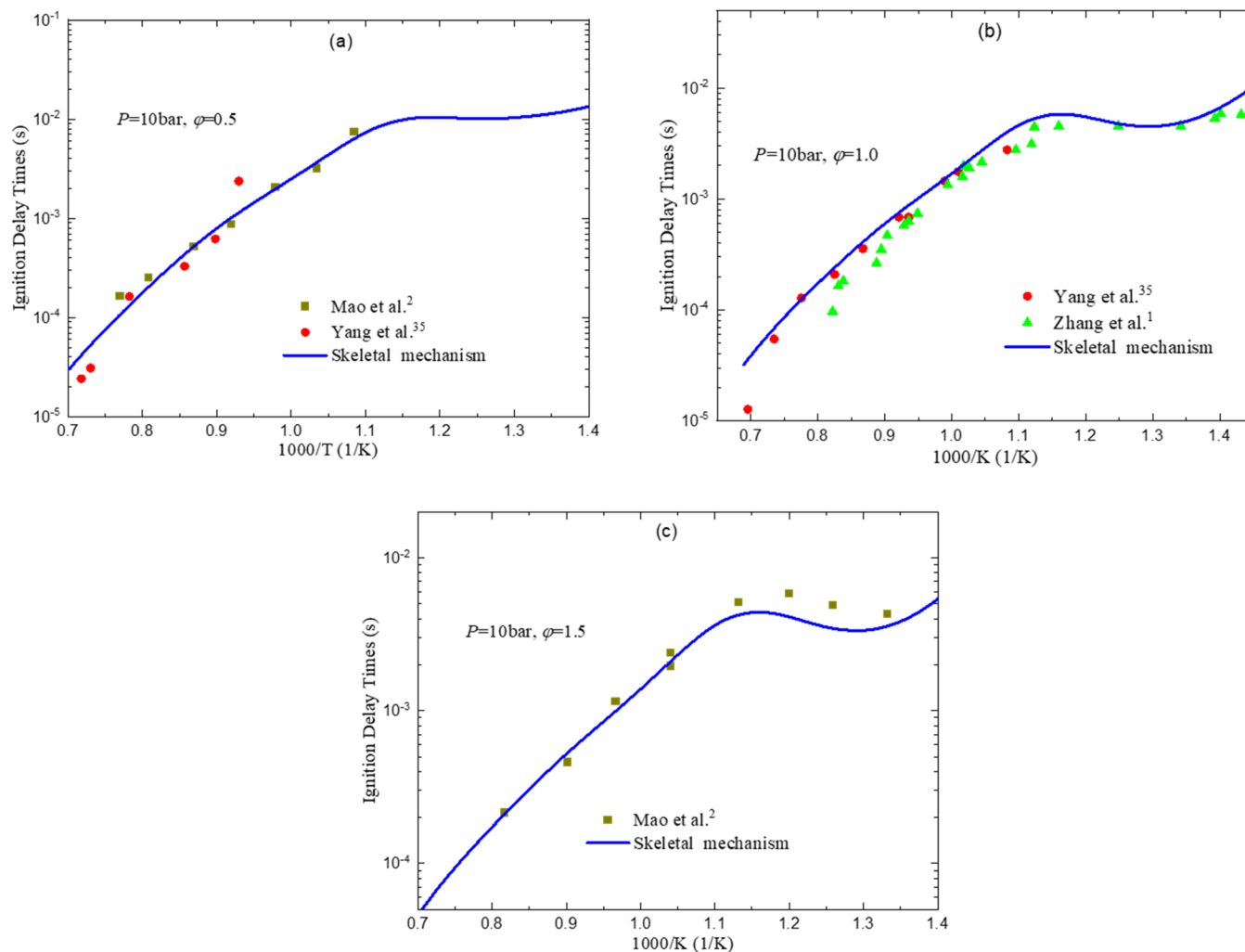


Figure 6. Comparison between the surrogate model predicted values and the experimental data of the ignition delay time for RP-3 fuel at $P = 10$ bar and equivalence ratios of (a) 0.5, (b) 1.0, and (c) 1.5. Symbols represent the experimental values.^{1,2,35} Solid lines represent the computational values of surrogate fuel.

5(a–d) clearly indicates that the predicted values of laminar flame speeds for four surrogate components are in excellent agreement with the experimental values.

4. SURROGATE FUEL MODEL VALIDATIONS AND DISCUSSION

In the previous section, the reliability of each component's skeletal mechanism was comprehensively verified. As a result, this section focuses on simulating the fundamental combustion characteristics of RP-3 fuel, including ignition delay time, species concentrations, and laminar flame speed, by combining the surrogate formulation and corresponding mechanism using the CHEMKIN software.²² The surrogate model predictions were extensively validated against experimental data in a subsequent section.

4.1. Validation of Ignition Delay Times. The ignition delay time was simulated based on the experimental conditions of Mao et al.,² Yang et al.,³⁵ and Zhang et al.¹ Figure 6 (a–c) displays the ignition characteristics of the RP-3 surrogate fuel mechanism at temperatures ranging from 650 to 1450 K and $\varphi = 0.5, 1.0,$ and $1.5,$ which were compared with the experimental values. For high-temperature conditions, the predicted values of the ignition delay time for the RP-3 surrogate mechanism

are in excellent agreement with the experimental values at all equivalence ratios. In the low-temperature region, the predicted ignition delay time of the RP-3 surrogate mechanism agrees well with the experimental data at $\varphi = 1.0$. However, at $\varphi = 1.5$, there is a slight undersizing in the prediction of the NTC phenomenon for the RP-3 fuel.

The sensitivity of the ignition delay time for the RP-3 surrogate mechanism was investigated, as depicted in Figure 7. The ignition delay time sensitivity coefficient was calculated under the conditions of $P = 20$ bar, $\varphi = 1$, and $T = 700$ and 1050 K, using the RP-3 surrogate fuel skeletal mechanism. Figure 7(a) reveals that in the low-temperature range, the isomerization of OOQOOH to generate ketone hydroperoxide and OH, as well as the decomposition of ketone hydroperoxide, exhibit the highest sensitivity. The dehydrogenation of the reaction “Decalin + OH = >RDecalin + H₂O” has a positive sensitivity coefficient and significantly inhibits ignition. Figure 7(b) demonstrates that at a temperature of 1050 K, the dehydrogenation reactions of base fuel $n\text{C}_{12}\text{H}_{26}$, C₈H₁₈-2S, and decalin with HO₂, the consumption reaction of CH₃, the cracking of C₄H₇-1, and the reaction of multiradical HO₂ to H₂O₂ exhibit the most sensitive response.

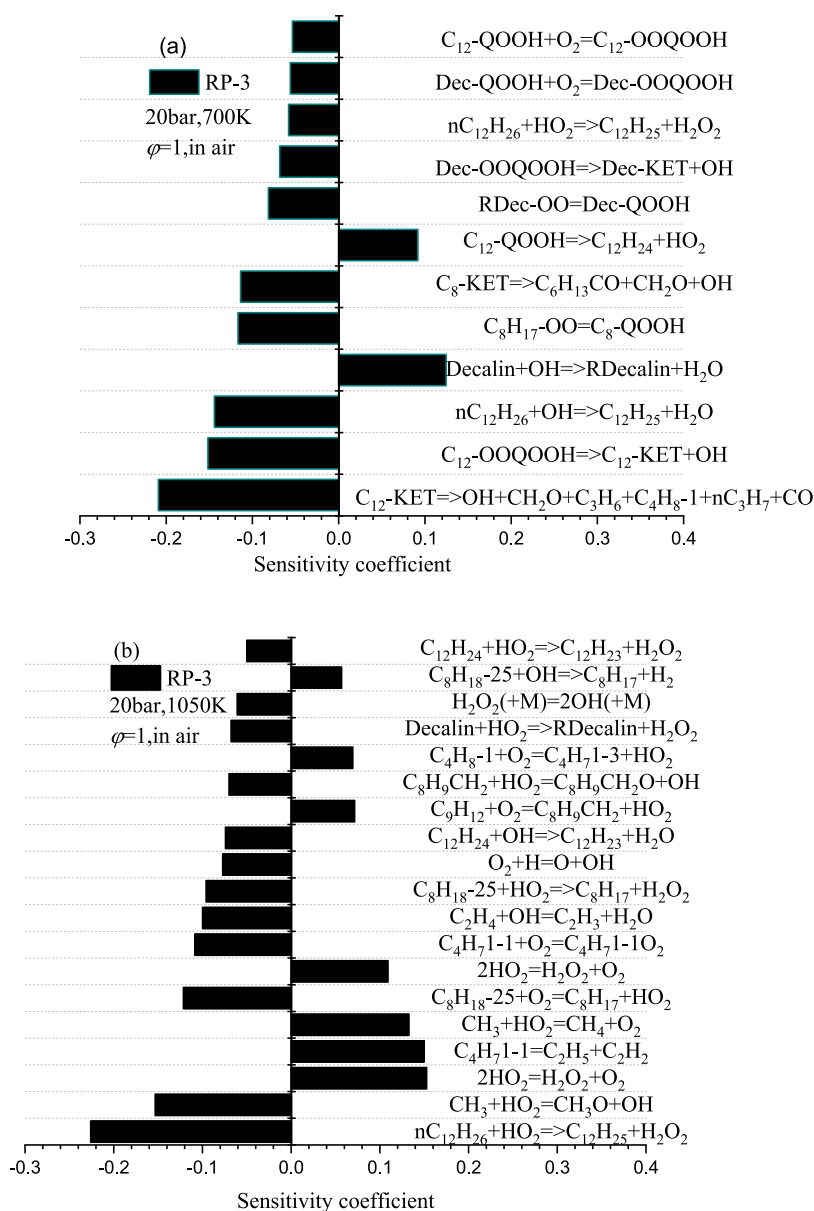


Figure 7. Sensitivity analysis of ignition delay time of RP-3 model fuel skeletal mechanism at $P = 20$ bar, $\varphi = 1.0$, $T = 700$ K (a) and $T = 1050$ K (b).

4.2. Validation of Species Concentrations. The oxidation of RP-3 fuel was investigated by Liu et al.⁸ using a jet stirred reactor (JSR) operating at $P = 1.0$ atm, $\varphi = 0.5$ and 1.0, temperatures ranging from 550 to 1100 K, and a residence time (τ) of 2.0 s. The partially stirred reactor (PSR) model was employed to simulate the concentration of the main species in the JSR. Figure 8 illustrates the comparisons between the surrogate simulations and experimental results of RP-3 fuel for initial reactants, major intermediate species, and products. The surrogate fuels for both $\varphi = 0.5$ (Figure 8(a),(b)) and 1.0 (Figure 8(c),(d)) can accurately predict the changes in concentrations of O_2 , H_2O , CO , CH_3OH , and CO_2 as the initial temperature increases. Notably, the surrogate fuel successfully captures the negative temperature coefficient (NTC) behavior observed in the concentration profiles of initial reactants, major intermediate species, and products from 600 to 700 K. Additionally, the surrogate fuel adequately captures the trend of H_2 and CH_4 concentrations but

overestimates the peak concentration of C_3H_6 in the low-temperature region. This is because only the parent fuel, oxidizers and products (CO_2 and H_2O), and the radicals of H , OH , HO_2 , CO , and CH_2O were employed as the reduction targets. Some paths dominating the formation of C_3H_6 might be deleted in the mechanism reduction process, which leads to discrepancies between the measured and calculated results. Overall, the RP-3 surrogate mechanism effectively predicts the oxidation characteristics of RP-3 fuel in the JSR.

4.3. Laminar Flame Speed Validation. The laminar flame speeds were calculated under various pressure and temperature conditions and compared to the experimental data,^{8,36} as shown in Figure 9. The results indicate that, for equivalent ratios $\varphi = 1.0$ to 1.4, the simulated values using the skeletal mechanism are in good agreement with the experimental values at all temperature conditions. However, within the range of equivalent ratio $\varphi = 0.6$ to 1.0 at $T = 420$ K, the simulated values using the skeletal mechanism are

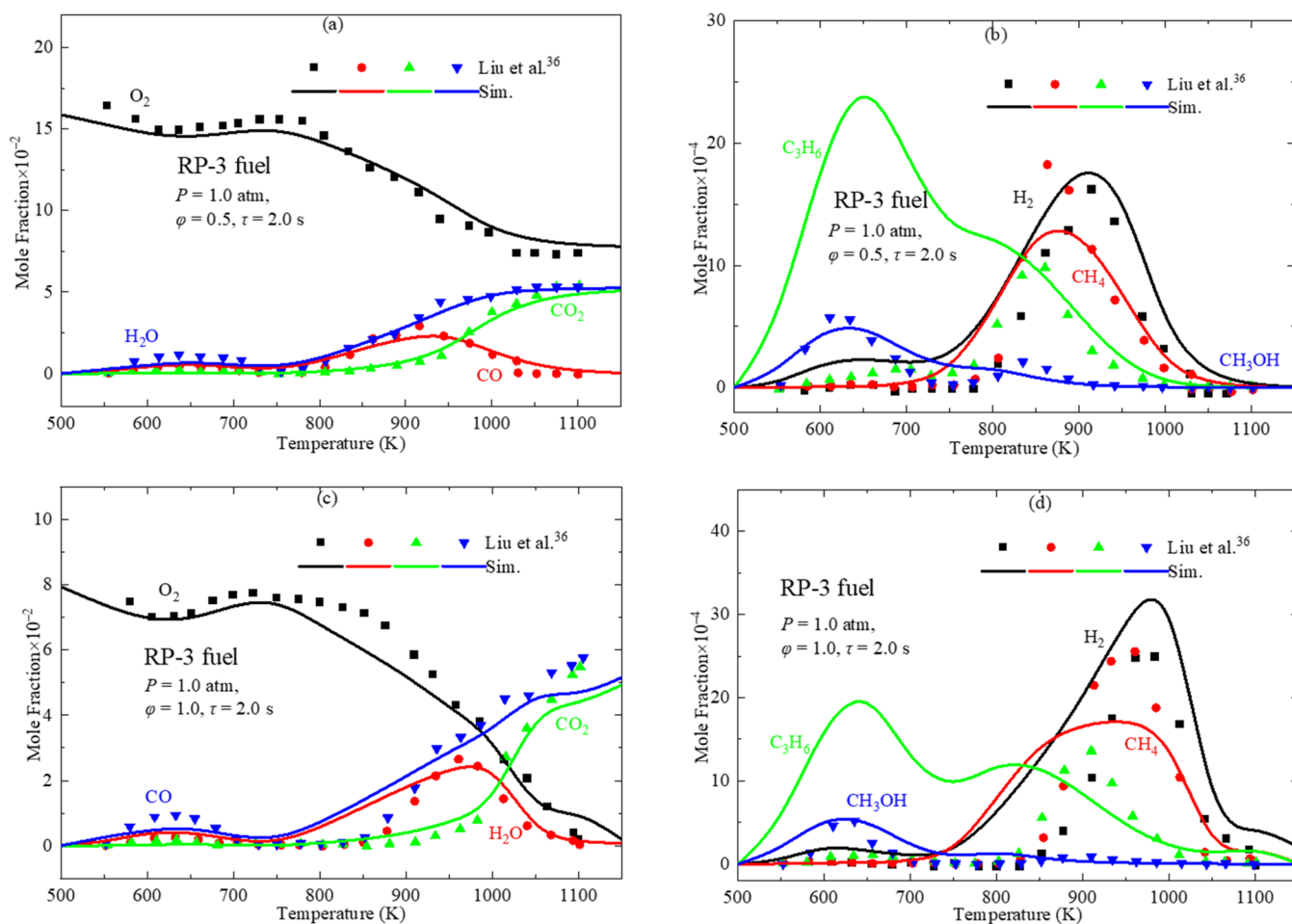


Figure 8. Comparison between the surrogate model predicted values and the experimental data of species concentration in the JSR for RP-3 fuel at equivalence ratios of (a, b) 0.5 and (c, d) 1.0. Symbols represent the experimental values.³⁶ Solid lines represent the computational values of the surrogate fuel.

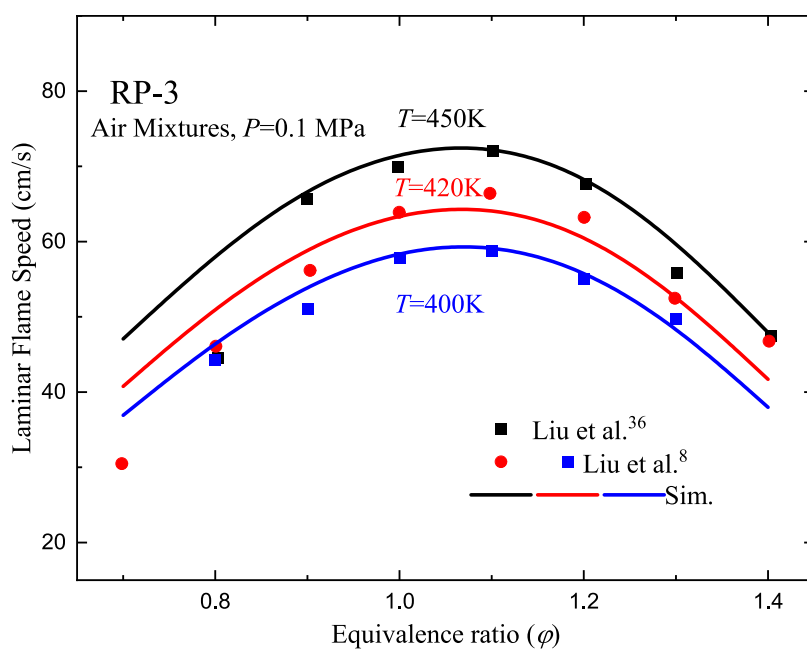


Figure 9. Comparison of laminar flame speed with experimental values^{8,36} for RP-3 model fuel skeletal mechanism at $P = 0.1$ MPa, $T = 400$, 420, and 450 K.

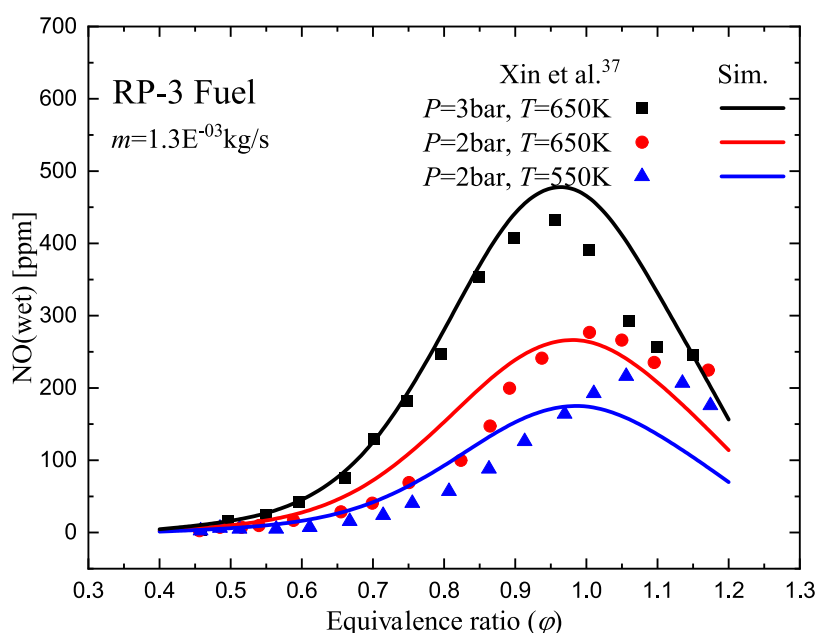


Figure 10. Comparison of the concentration change of NO with experimental values³⁷ at different equivalent ratios.

slightly higher than the experimental values. Additionally, at a temperature of $T = 400$ K, the simulated values using the skeletal mechanism accurately match the experimental data across a wide range of equivalence ratios. In conclusion, the four-component surrogate fuel skeletal mechanism proves to be an effective predictor of the laminar flame speed for the RP-3 fuel.

4.4. Verification of NO Formation Mechanism. To investigate the NO_x emissions of the RP-3 surrogate fuel under different pressure and temperature conditions, the experimental data from the literature³⁷ were utilized, as shown in Figure 10. The experiment was conducted in a jet stirred combustion reactor, with the following parameters: a total flow rate (m) of 1.3×10^{-3} kg/s for the premixed gas, τ ranging from 4.4 to 12 ms, controlled inlet temperatures (T_{in}) of 550 and 650 K, varying ϕ from 0.4 to 1.2, and pressure inside the agitator set at 2 and 3 bar, respectively. As shown in Figure 10, the calculated emissions agreed well with the experimental results at different pressures and inlet temperatures. However, under $P = 2$ bar and $T_{\text{in}} = 550$ K, a slight shift to a lower equivalence ratio was observed in the calculated NO_x production. This is mainly limited by the precision of the NO_x mechanism of GRI 3.0.

5. CONCLUSIONS

- (1) A novel methodology for developing skeletal mechanism by combining the detailed C_0 – C_4 mechanism and C_5 – C_n high-carbon molecular skeletal mechanism was proposed in this study. This methodology combines the compactness of the decoupling methodology with the high accuracy of the updated decoupling methodology.
- (2) A refined RP-3 fuel skeletal mechanism was developed using the proposed methodology. This mechanism consists of 153 species and 858 reactions. The verification results indicate that the developed RP-3 fuel skeletal mechanism performs well in predicting the ignition delay time, species oxidation concentration, and laminar flame speed of each component and RP-3 fuel.

Furthermore, the model fuel mechanism accurately predicts the NO and CO emissions of RP-3 fuel.

- (3) The strong agreement observed between the simulation and experimental results validates the compactness and accuracy of the innovative methodology proposed in this study. Furthermore, it offers a practical approach for elucidating the mechanisms underlying high-carbon model fuels.

■ ASSOCIATED CONTENT

Supporting Information

The Supporting Information is available free of charge at <https://pubs.acs.org/doi/10.1021/acsomega.3c05087>.

Skeletal mechanism, thermodynamic data, and transport data for surrogate fuel (PDF)

■ AUTHOR INFORMATION

Corresponding Author

Jin Yu – School of Aeronautics, Chongqing Jiaotong University, Chongqing 400074, China; The Green Aerotechnics Research Institute of Chongqing Jiaotong University, Chongqing 401120, China; Chongqing Key Laboratory of Green Aviation Energy and Power, Chongqing 401120, China; School of Mechatronics & Vehicle Engineering, Chongqing Jiaotong University, Chongqing 400074, China; orcid.org/0000-0001-5695-6886; Email: yjin123@yeah.net

Authors

Ping Liu – School of Aeronautics, Chongqing Jiaotong University, Chongqing 400074, China; The Green Aerotechnics Research Institute of Chongqing Jiaotong University, Chongqing 401120, China; Chongqing Key Laboratory of Green Aviation Energy and Power, Chongqing 401120, China
 Xiangkui Gong – School of Mechatronics & Vehicle Engineering, Chongqing Jiaotong University, Chongqing 400074, China

Tao Deng – School of Aeronautics, Chongqing Jiaotong University, Chongqing 400074, China; The Green Aerotechnics Research Institute of Chongqing Jiaotong University, Chongqing 401120, China; Chongqing Key Laboratory of Green Aviation Energy and Power, Chongqing 401120, China; orcid.org/0000-0001-6881-9854

Complete contact information is available at:

<https://pubs.acs.org/10.1021/acsomega.3c05087>

Notes

The authors declare no competing financial interest.

ACKNOWLEDGMENTS

This work was supported by National Natural Science Foundation of China (nos. 52006020 and 52275051), Science and Technology Research Program of Chongqing Municipal Education Commission (grant no. KJQN202000721), and Key Projects of Technological Innovation and Application Development of Chongqing (grant no. cstc2019jscx-fxydX0028).

REFERENCES

- (1) Zhang, C.; Li, B.; Rao, F.; Li, P.; Li, X. A shock tube study of the autoignition characteristics of RP-3 jet fuel. *Proc. Combust. Inst.* **2015**, *35* (3), 3151–3158.
- (2) Mao, Y.; Yu, L.; Wu, Z.; Tao, W.; Wang, S.; Ruan, C.; Zhu, L.; Lu, X. Experimental and kinetic modeling study of ignition characteristics of RP-3 kerosene over low-to-high temperature ranges in a heated rapid compression machine and a heated shock tube. *Combust. Flame* **2019**, *203*, 157–169.
- (3) Dong, Z.; Yu, W.-M.; Zhong, B.-J. RP-3 aviation kerosene surrogate fuel and the chemical reaction kinetic model. *Acta Phys.-Chim. Sin.* **2015**, *31* (4), 636–642.
- (4) Zeng, W.; Li, H.-x.; Chen, B.-d.; Ma, H.-a. Experimental and kinetic modeling study of ignition characteristics of Chinese RP-3 kerosene. *Combust. Sci. Technol.* **2015**, *187* (3), 396–409.
- (5) Liu, Y.; Liu, Y.; Chen, D.; Fang, W.; Li, J.; Yan, Y. A simplified mechanistic model of three-component surrogate fuels for RP-3 aviation kerosene. *Energy Fuels* **2018**, *32* (9), 9949–9960.
- (6) Ranzi, E.; Frassoldati, A.; Stagni, A.; Pelucchi, M.; Cuoci, A.; Faravelli, T. Reduced kinetic schemes of complex reaction systems: fossil and biomass-derived transportation fuels. *Int. J. Chem. Kinet.* **2014**, *46* (9), 512–542.
- (7) Liu, X.; Wang, Y.; Bai, Y.; Zhou, Q.; Yang, W. Development and verification of a physical–chemical surrogate model of RP-3 kerosene with skeletal mechanism for aircraft SI engine. *Fuel* **2022**, *311*, No. 122626.
- (8) Liu, J.; Hu, E.; Yin, G.; Huang, Z.; Zeng, W. An experimental and kinetic modeling study on the low-temperature oxidation, ignition delay time, and laminar flame speed of a surrogate fuel for RP-3 kerosene. *Combust. Flame* **2022**, *237*, No. 111821.
- (9) Chang, Y.; Jia, M.; Li, Y.; Liu, Y.; Xie, M.; Wang, H.; Reitz, R. D. Development of a skeletal mechanism for diesel surrogate fuel by using a decoupling methodology. *Combust. Flame* **2015**, *162* (10), 3785–3802.
- (10) Dooley, S.; Won, S. H.; Chaos, M.; Heyne, J.; Ju, Y.; Dryer, F. L.; Kumar, K.; Sung, C.-J.; Wang, H.; Oehlschlaeger, M. A.; et al. A jet fuel surrogate formulated by real fuel properties. *Combust. Flame* **2010**, *157* (12), 2333–2339.
- (11) Zhang, X.; Sarathy, S. M. A lumped kinetic model for high-temperature pyrolysis and combustion of 50 surrogate fuel components and their mixtures. *Fuel* **2021**, *286*, No. 119361.
- (12) Yu, J.; Ju, Y.; Gou, X. Surrogate fuel formulation for oxygenated and hydrocarbon fuels by using the molecular structures and functional groups. *Fuel* **2016**, *166*, 211–218.
- (13) Yu, J.; Cao, J.-m.; Yu, J.-j. The development of F-76 and algae-derived HRD-76 diesel fuel surrogates. *Fuel* **2021**, *302*, No. 121075.
- (14) Yu, J.; Wang, Z.; Zhuo, X.; Wang, W.; Gou, X. Surrogate definition and chemical kinetic modeling for two different jet aviation fuels. *Energy Fuels* **2016**, *30* (2), 1375–1382.
- (15) Yu, B.; Jiang, X.; He, D.; Wang, C.; Wang, Z.; Cai, Y.; Yu, J.; Yu, J.-j. Development of a Chemical-Kinetic Mechanism of a Four-Component Surrogate Fuel for RP-3 Kerosene. *ACS Omega* **2021**, *6* (36), 23485–23494.
- (16) Smith, G. P.; Golden, D. M.; Frenklach, M.; Moriarty, N. W.; Eiteneer, B.; Goldenberg, M.; Bowman, C. T.; Hanson, R. K.; Song, S.; Gardiner, W., Jr. GRI-Mech 3.0 2011 http://www.me.berkeley.edu/gri_mech38.
- (17) Fang, X.; Huang, X.; Chen, W.; Qiao, X.; Ju, D. Development of a skeletal surrogate mechanism for emulating combustion characteristics of diesel from direct coal liquefaction. *Combust. Flame* **2020**, *218*, 84–97.
- (18) Bao, Y.; Du, H.; Chai, W. S.; Nie, D.; Zhou, L. Numerical investigation and optimization on laminar burning velocity of ammonia-based fuels based on GRI3.0 mechanism. *Fuel* **2022**, *318*, No. 123681.
- (19) Pepiot-Desjardins, P.; Pitsch, H. An efficient error-propagation-based reduction method for large chemical kinetic mechanisms. *Combust. Flame* **2008**, *154* (1–2), 67–81.
- (20) Stagni, A.; Frassoldati, A.; Cuoci, A.; Faravelli, T.; Ranzi, E. Skeletal mechanism reduction through species-targeted sensitivity analysis. *Combust. Flame* **2016**, *163*, 382–393.
- (21) Curtis, N. J.; Niemeyer, K. E.; Sung, C. J. An automated target species selection method for dynamic adaptive chemistry simulations. *Combust. Flame* **2015**, *162* (4), 1358–1374.
- (22) Chemkin. 2000 <http://www.reactiondesign.com/products/chemkin>.
- (23) Shen, H.-P. S.; Steinberg, J.; Vanderover, J.; Oehlschlaeger, M. A. A Shock Tube Study of the Ignition of n-Heptane, n-Decane, n-Dodecane, and n-Tetradecane at Elevated Pressures. *Energy Fuels* **2009**, *23* (3), 2482–2489.
- (24) Oehlschlaeger, M. A.; Shen, H.; Frassoldati, A.; Pierucci, S.; Ranzi, E. Experimental and Kinetic Modeling Study of the Pyrolysis and Oxidation of Decalin. *Energy Fuels* **2009**, *23*, 1464–1472.
- (25) Zhu, Y.; Davidson, D. F.; Hanson, R. K. Pyrolysis and oxidation of decalin at elevated pressures: A shock-tube study. *Combust. Flame* **2014**, *161* (2), 371–383.
- (26) Sarathy, S. M.; Javed, T.; Karsenty, F.; Heufer, A.; Wang, W.; Park, S.; Elwardany, A.; Farooq, A.; Westbrook, C. K.; Pitz, W. J.; et al. A comprehensive combustion chemistry study of 2,5-dimethylhexane. *Combust. Flame* **2014**, *161* (6), 1444–1459.
- (27) Diévar, P.; Kim, H. H.; Won, S. H.; Ju, Y.; Dryer, F. L.; Dooley, S.; Wang, W.; Oehlschlaeger, M. A. The combustion properties of 1,3,5-trimethylbenzene and a kinetic model. *Fuel* **2013**, *109*, 125–136.
- (28) Mzè-Ahmed, A.; Hadj-Ali, K.; Dagaut, P.; Dayma, G. Experimental and Modeling Study of the Oxidation Kinetics of n-Undecane and n-Dodecane in a Jet-Stirred Reactor. *Energy Fuels* **2012**, *26* (7), 4253–4268.
- (29) Gudiyella, S.; Brezinsky, K. High pressure study of 1,3,5-trimethylbenzene oxidation. *Combust. Flame* **2012**, *159* (11), 3264–3285.
- (30) Dagaut, P.; Ristori, A.; Frassoldati, A.; Faravelli, T.; Dayma, G.; Ranzi, E. Experimental and semi-detailed kinetic modeling study of decalin oxidation and pyrolysis over a wide range of conditions. *Proc. Combust. Inst.* **2013**, *34* (1), 289–296.
- (31) Ji, C.; Dames, E.; Wang, Y. L.; Hai, W.; Egolfopoulos, F. N. Propagation and extinction of premixed C5–C12 n-alkane flames. *Combust. Flame* **2010**, *157* (2), 277–287.
- (32) Ji, C.; Sarathy, S. M.; Veloo, P. S.; Westbrook, C. K.; Egolfopoulos, F. N. Effects of fuel branching on the propagation of octane isomers flames. *Combust. Flame* **2012**, *159* (4), 1426–1436.

(33) Comandini, A.; Dubois, T.; Abid, S.; Chaumeix, N. Comparative Study on Cyclohexane and Decalin Oxidation. *Energy Fuels* **2014**, *28* (1), 714–724.

(34) Bo, L.; Hai, Z.; Egolfopoulos, F. N. Laminar flame propagation of atmospheric iso-cetane/air and decalin/air mixtures. *Combust. Flame* **2014**, *161* (1), 154–161.

(35) Yang, Z. Y.; Zeng, P.; Wang, B. Y.; Jia, W.; Xia, Z.-X.; Liang, J.; Wang, Q. D. Ignition characteristics of an alternative kerosene from direct coal liquefaction and its blends with conventional RP-3 jet fuel. *Fuel* **2021**, *291* (14), No. 120258.

(36) Liu, Y.; Wang, J.; Gu, W.; Ma, H.; Zeng, W. An Experiment Study on the Laminar Burning Velocity and Markstein Length of Chlorella Oil/RP3 Kerosene Blends. *ACS Omega* **2020**, *5* (37), 23510–23519.

(37) Xin, X.; Lin, Y.; Chi, Z.; Ye, T.; Sung, C. J. In *Experimental Study on NO_x and CO Emissions of Aviation Kerosene and Coal-to-Liquid Synthetic Aviation Fuel in a Jet Stirred Combustion Reactor*, Asme Turbo Expo: Turbine Technical Conference & Exposition ; ASME, 2014.